J Mol Model (2013) 19:83–95
DOI 10.1007/s00894-012-1521-1

ORIGINAL PAPER

A DFT study on the mechanisms for the cycloaddition reactions between 1−aza-2-azoniaallene cations and acetylenes

Jing-mei Wang · Zhi-ming Li · Quan-rui Wang · Feng-gang Tao

Received: 11 April 2012 / Accepted: 26 June 2012 / Published online: 19 July 2012

Abstract The mechanisms of cycloaddition reactions between 1-aza-2-azoniaallene cations **1** and acetylenes **2** have been investigated using the global electrophilicity and nucleophilicity of the corresponding reactants as global reactivity indexes defined within the conceptual density functional theory. The reactivity and regioselectivity of these reactions were predicted by analysis of the energies, geometries, and electronic nature of the transition state structures. The theoretical results revealed that the reaction features a tandem process: an ionic 1,3-dipolar cycloaddition to produce the cycloadducts 3 *H*-pyrazolium salts **3** followed by a [1,2]-shift affording the thermodynamically more stable adducts **4** or **5**. The mechanism of the cycloaddition reactions can be described as an asynchronous concerted pathway with reverse electron demand. The model reaction has also been investigated at the QCISD/6-31++G(d,p) and CCSD(T)/6-31++G(d,p)//B3LYP/6-31++G(d,p) levels as well as by the DFT. The polarizable continuum model, at the B3LYP/6-31++G(d,p) level of theory, was used to study solvent effects on all the studied reactions. In solvent dichloromethane, all the initial cycloadducts **3** were obtained via direct ionic process as the result of the solvent effect. The consecutive [1,2]-shift reaction, in which intermediates **3** are rearranged to the five-membered heterocycles **4**/**5**, is proved to be a kinetically controlled reaction, and the regioselectivity can be modulated by varying the migrant. The LOL function and RDG function based on localized electron analysis were used to analysis the covalent bond and noncovalent interactions in order to unravel the mechanism of the title reactions.

Keywords Acetylenes · 1-aza-2-azoniaallene cations · Cycloaddition · Density functional calculations · Reaction mechanism

Abbreviations

B3LYP	Becke-3-parameter-Lee-Yang-Parr
QCISD	Quadratic configuration interaction using single and double substitutions
CCSD(T)	Coupled cluster calculations with single and double excitations and a perturbative estimate of triple contributions
DFT	Density functional theory
PCM	Polarized continuum model
IRC	Intrinsic reaction coordinate
NBO	Natural bond orbital
LOL	Localized orbital locator
RDG	Reduced density gradient
AM1	Austin model 1

Introduction

The 1,3-dipolar cycloaddition, also known as the Huisgen cycloaddition or Huisgen reaction, is the reaction of a dipolarophile with a 1,3-dipolar compound that leads to 5-membered (hetero)cycles. Many of these kinds of reactions take place with high regio- as well as stereoselectivity, and the process has proved to be a very useful and versatile methodology in synthetic organic chemistry [1–5]. Since the classification and systematization by Huisgen in the

Electronic supplementary material The online version of this article (doi:10.1007/s00894-012-1521-1) contains supplementary material, which is available to authorized users.

J.-m. Wang · Z.-m. Li (✉) · Q.-r. Wang · F.-g. Tao
Department of Chemistry, Fudan University,
Shanghai 200433, People's Republic of China
e-mail: zmli@fudan.edu.cn

J.-m. Wang
Research Centre for Analysis & Measurement, Fudan University,
Shanghai 200433, People's Republic of China

1960s [1], considerable experimental [6–8] and theoretical [9–12] work has been done to address the vast synthetic utilities as well as the mechanistic aspects. Many theoretical investigation indicated that 2π-electrons of the dipolarophile and 4π-electrons of the dipolar reactant participate in a concerted, pericyclic process [13–15], similar to the Diels-Alder reaction. However, the study has mainly been restricted to neutral 1,3-dipolar cycloaddition.

Since the 1990s, the cationic four-electron, three-center components, *i.e.*, 1-aza-2-azoniaallene cations have aroused considerable attention in the domain of synthetic chemistry. With multiple bond compounds, they behave as positively charged dipoles to furnish various nitrogen-containing five-membered heterocycles. Compared with neutral 1,3-dipoles, these positively charged 1,3-dipoles are unique with respect to the generation, reaction pattern and the favorability on the 1,3-dipolarophiles. Moreover, the inherent transient cationic nature of the initial adducts allows for a facile consecutive shift reaction, which widens the structural diversities of the 5-membered heterocycles.

The 1-aza-2-azoniaallene cations, also described as azocarbenium ions, are usually generated as short-lived reactive intermediates in many oxidative processes of hydrazones or obtained from α-chloroalkyl azo compounds by treatment with Lewis acids such as $SbCl_5$ or $AlCl_3$ at low temperatures [16, 17]. The 1,3-dipolar cycloaddition of 1-aza-2-azoniaallene cations with multiple bonds, such as nitriles [16, 18], olefins [19, 20], acetylenes [21, 22], carbodiimides [23, 24] and isocyanates [25, 26], have been well exploited. Parallel to the experimental findings[4, 8, 27], some semi-empirical AM1 calculations [16, 19, 22, 23, 25] have also been carried out to illuminate the mechanism by Wang et al. During the past decades, high-level calculations on this issue have aroused chemist's interest and 1,3-dipolar cycloaddition reactions between 1-aza-2-azoniaallene cations and olefins [20] as well as isocyanates [26] have been theoretically investigated by Fang and co-workers.

We also have been engaged in a program aimed at unraveling the mechanistic mystery of the 1,3-dipolar cycloadditions involving an azocarbenium ion as the dipole molecule. Working in this line, we have accomplished the theoretical study on the 1,3-dipolar cycloaddition of 1-aza-2-azoniaallene cations with nitriles [18] and carbodiimides [24] using the DFT.

It is well known that, acetylene is a common chemical reactant acting as effective electrophilic dipolarophile. However, due to the much enhanced electrophilicity of 1-aza-2-azoniaallene cations, acetylenes behave as nucleophiles to undergo this kind of 1,3-dipolar cycloaddition with subsequent [1,2]-shift to afford 1*H*-pyrazolium salts or 4*H*-pyrazolium salts or mixtures of both [22]. Herein, we wish to report our theoretical study on the mechanism, solvent and substituent effects of the title reaction using high level theoretical calculation. The studied reactions are shown in Scheme 1.

Computational methods

All theoretical calculations were performed with Gaussian 09 program package, revision A.02 [28]. The geometries of reactants, products, precursor complexes, and transition states were fully optimized at the B3LYP method of DFT using 6-31++G(d,p) basis set and characterized by the number of imaginary frequencies. For all the reaction paths, the IRC [29, 30] was traced to confirm the TS connecting with the corresponding two minima. The geometries of the reactants, complexes, transition states, and products of the model reaction were also optimized at QCISD method [31, 32] using 6-31++G(d,p) basis set. To obtain more reliable energies, single-point CCSD(T) [33, 34] were carried out with all the stationary points in the model reaction, which were optimized at B3LYP/6-31++G(d,p) level. For the title reaction, the effect of solvation on reaction energetics was determined by single-point calculations at the same level on the gas-phase optimized geometries. The PCM [35–38] that builds the molecular surface starting from atomic radii (UFF), implemented in Gaussian 09 package was used and the calculation is performed at the reaction temperature. CH_2Cl_2 was chosen as the model solvent with a relative

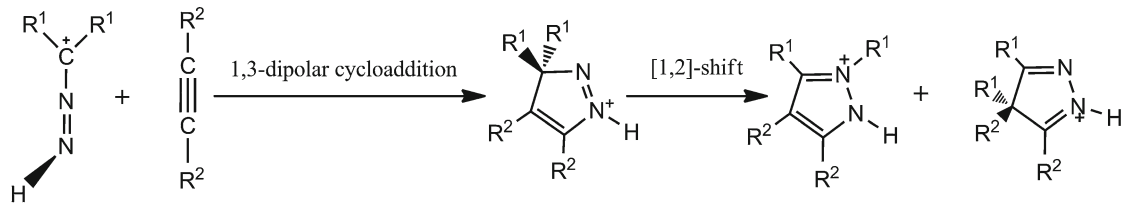

R1a:R^1=H **R2a**: R^2=H
R1b:R^1=Me **R2b**: R^2=Me
R1c:R^1=Cl **R2c**: R^2=Cl

3a:R^1=H, R^2=H
3b:R^1=Me, R^2=H
3c:R^1=Cl, R^2=H
3d:R^1=H, R^2=Me
3e:R^1=H, R^2=Cl

4a:R^1=H, R^2=H
4b:R^1=Me, R^2=H
4c:R^1=Cl, R^2=H
4d:R^1=H, R^2=Me
4e:R^1=H, R^2=Cl

5a:R^1=H, R^2=H
5b:R^1=Me, R^2=H
5c:R^1=Cl, R^2=H
5d:R^1=H, R^2=Me
5e:R^1=H, R^2=Cl

Scheme 1 The reactions between azocarbenium ions and acetylenes

permittivity of 8.93. PCM with B3LYP geometries are known to yield results closer to the experimental result.

The model 1,3-dipolar cycloaddition reaction was analyzed using the global indexes [39–42], as defined within the context of DFT, which are useful tools to understand the reactivity of molecules in their ground states. Wherein, the electronic chemical potential (μ) is usually associated with the charge transfer ability of the system in its ground state geometry. The chemical hardness (η) is considered to be a measure of the stability of a system. The global electrophilicity (ω) encompasses both μ and η and measures the stabilization in energy when the system acquires an additional electronic charge from the environment. It has also frequently proved to be a useful indicator for predicting chemical reactivity. The global nucleophilicity (N) is an empirical (relative) nucleophilicity which was introduced by Domingo in 2008 and takes tetracyanoethylene (TCE) as a reference [43].

The NBO program in Gaussian 09, Version 5.9 [44], was used to obtain more information about some special bonds [45, 46]. LOL [47–50] and RDG [51] based on localized electron analysis have been used to study the covalent bond and noncovalent interactions for some stationary points in the studied reactions. Multiwfn package, revision 2.1 [52], has been employed for LOL and RDG analysis using the wavefunction obtained from the B3LYP/6-31++G(d,p) calculation.

Results and discussion

The title reactions between 1-aza-2-azoniallene cations and acetylenes have been examined using B3LYP/6-31++G(d,p) level of theory. Based on the calculation, the reaction is a typical tandem reaction that comprises two consecutive processes, which is similar to the results found in the cycloadditions with other dipolarophiles (nitriles, carbodiimides, olefins and isocyanates) [18, 20, 24, 26]. The first step is an ionic 1,3-dipolar cycloaddition proceeding spontaneously to yield the cycloadduct **3** without acquiring external energy, which is in good agreement with the experimental finding, described by Wang et al. in 1994, that cycloaddition of 1-aza-2-azoniaalene salts with acetylenes occurred at −60 °C [22]. The next step is a [1,2]-shift reaction of cycloadduct **3** to produce the thermodynamically more stable heterocycle **4** or **5**. For the second step, a much higher activation barrier has to be overcome than that required for the cycloaddition reaction, which is also consistent with the experimental findings in the same article by Wang et al., that the [1,2]-shift reaction occurred when the mixture had been warmed to 0 °C [22]. It indicates that the [1,2]-shift reaction should be the rate-determining step of the title reaction. Thereinafter, we will discuss the two consecutive reactions respectively, and focus mostly on the mechanism of the 1,3-dipolar cycloaddition reaction and the substituent effect of the [1,2]-shift which has been proved to control the distribution of the final products **4**/**5** reported by Wang et al. in 1994 [22].

The cationic 1,3-dipolar cycloaddition reactions

In this section, we tried to investigate the model 1,3-dipolar cycloaddition reaction (**R1a** + **R2a**, Reaction **a** in Scheme 1) and the corresponding substituent effects of the azocarbenium ion as well as acetylene both in the gas phase and in dichloromethane. The geometries of the reactants (**R1** and **R2**), complexes (**COM**), transition states (**TS13**), and products (**3**) were optimized at B3LYP/6-31++G(d,p) level and the optimized parameters, energies, and frequencies of these stationary points are provided in Tables S1-S2, S3 and S9 of the online resource 1.

The model 1,3-dipolar cycloaddition reaction

The model reaction was first investigated in the gas phase. Figure 1 provides the optimized geometries and atomic numbering systems of all the stationary points (more detailed information is given in Fig. S1 of the online resource 2). Based on the B3LYP/6-31++G(d,p) calculation, the skeleton atoms of the 1-aza-2-azoniaallene cation (**R1a**) adopts a linear geometry with the hydrogen atom connected with the nitrogen atom in the same plane (H4-N1-N2-C3=180.0°), while the plane of the methylene group is essentially perpendicular to the C3-N2-N1 plane with the dihedral angle (H5-C3-N2-N1) being 91.0° [18, 20, 24, 26]. Not surprisingly, another reactant, acetylene (**R2a**) is also a linear molecule with two *sp* hybridized C atoms.

As quoted in Table 1, the difference between electronic chemical potential values (μ) of cation **R1a** and acetylenes **R2a** is a significant gap (-0.31 a.u. for the model reaction) which is in accord with the distinct charges in the two reactants. Owing to the favorable electrostatic interaction of the reactants, a net charge transfer is expected to take place from **R1a** to **R2a**. Although the chemical potential allows us to correctly establish the directionality of the charge transferring, the reactions may be better visualized by using the electrophilicity index (ω) that concurrently incorporates the resistance to the electron charge to be deformed (e.g., hardness). Acetylene (**R2a**), with a low electrophilicity value (ω=0.97 eV), is generally classified as a moderate electrophile within the electrophilicity scale, while it presents as a nucleophile in this reaction because of the rather high electrophilicity (ω=13.70 eV) of **R1a**. Taking into account the great $\Delta\omega$ value of 12.73 eV between **R1a** and **R2a**, this reaction is expected to exhibit, if not definitely ionic, a very typical polar character [53]. It means that the 1,3-dipolar cycloaddition reaction of the

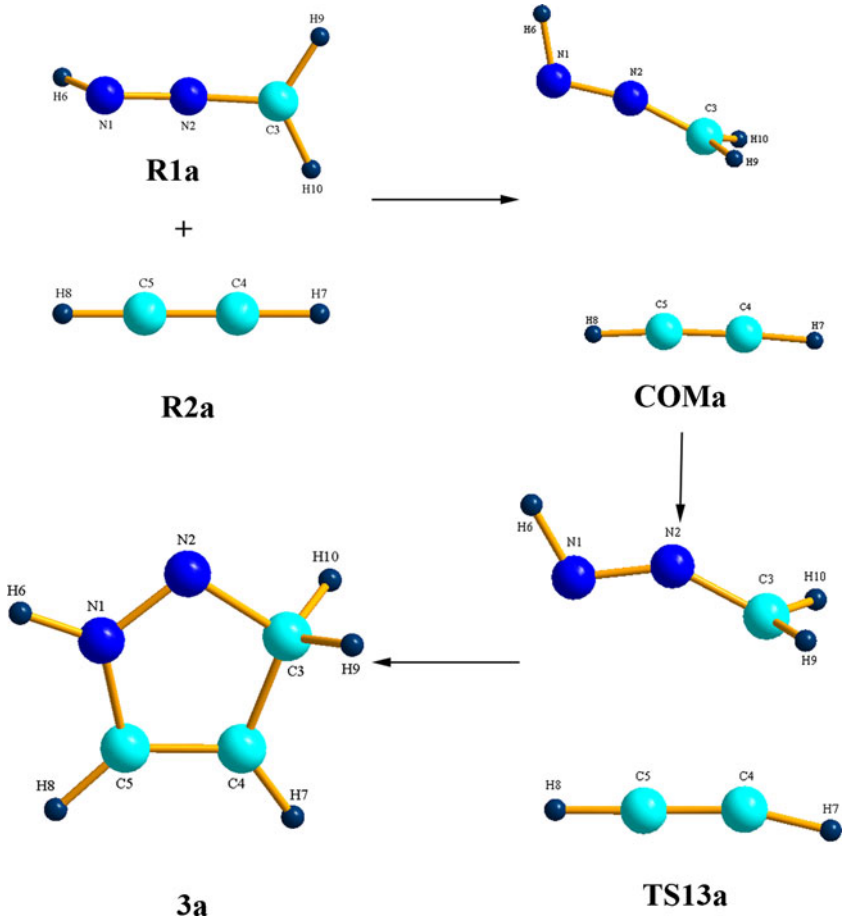

Fig. 1 Optimized geometries (B3LYP/6-31++G(d,p)) and atomic numbering systems of all the stationary points in the model 1,3-dipolar cycloaddition reaction

model reaction proceeds via an initial nucleophilic attack of the acetylenes **R2a** on the highly activated cation **R1a**.

When reactants (**R1a** + **R2a**) approach each other, as shown in Fig. 1, a complex with noncovalent interaction denoted as **COMa** is formed. After that, a concerted pathway for the cycloaddition can be observed: **COMa** is destroyed to afford the 3*H*-pyrazolium ion **3a** via **TS13a** directly. From the structural parameters along the concerted process, it can be seen that the skeleton atoms (N1-N2-C3-C4-C5) of both **COMa** and **TS13a** are in the same plane (dihedral angles N1-N2-C4-C5 are 0.0°) which is quite similar to the geometry of the initial product **3a**. It infers that approaching in coplanar mode should be propitious to form **3a** along the concerted process. Considering the huge $\Delta\omega$ between **R1a** and **R2a**, the reaction can be classified as a "1,3-dipolar cycloaddition with reverse electron demand", denoted as "type III" according to Sustmann's classification [54]. For RDG analysis (Fig. 2), there is only one area of lower density surface between C3 and C4 in **COMa**, where the weak electrostatic attractiveness between the approaching atoms is expected. The lengths of the two forming bonds in **COMa** are 3.088 Å (C3-C4) and 4.185 Å (N1-C5), and the angle of the skeleton atoms (N1-N2-C3) turns to be 165.4° from the original 170.7° (**R1a**). With the reaction progression, the skeleton atoms in **TS13a** (N1-N2-C3= 144.1°) become more bent, thus the two set of active sites (N1-C5 and C3-C4) approach closer (C3-C4=2.442 Å, N1-C5=3.030 Å). These are also in line with the RDG analysis, as shown in Fig. 2. The density of isosurface lying between C3 and C4 increases and another lower density surface between N1 and C5 expresses. This indicates that the interactions between the reactant fragments in **TS13a** have strong electrostatic attraction for C3 and C4, weak electrostatic attraction for N1 and C5 and weak repulsion close to

Table 1 Global properties (electronic chemical potential μ in au; chemical hardness η values in au; electrophilicity power ω in eV; global nucleophilicity N, values in eV) of reactants at B3LYP/6-31++G(d,p) level

Reactant	μ(au)	η(au)	ω(eV)	N(eV)
R1a	−0.46	0.209	13.70	−5.55
R1b	−0.41	0.191	11.76	−3.87
R1c	−0.43	0.158	16.09	−4.15
R2a	−0.15	−0.301	0.97	1.89
R2b	−0.14	−0.264	1.02	2.78
R2c	−0.15	−0.273	1.08	1.29

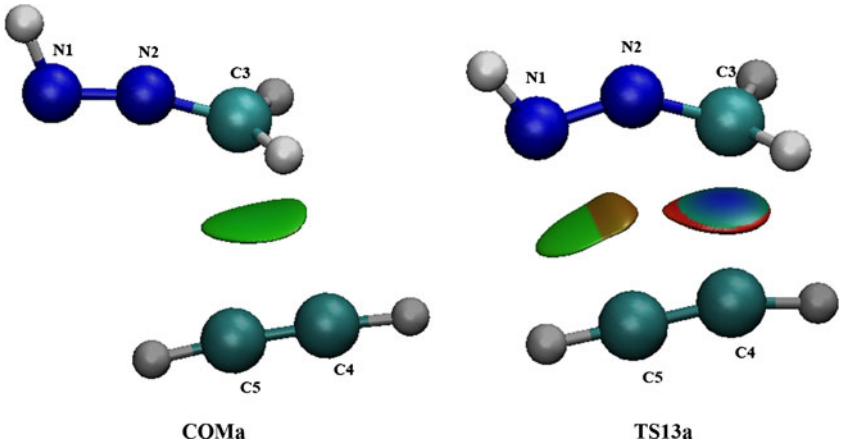

Fig. 2 Optimized geometries (B3LYP/6-31++G(d,p)) and gradient isosurfaces (s=1/2 a.u.) for (**a**) **COMa**, (**b**) **TS13a**. The surfaces are colored on a blue-green-red scale according to values of sign (λ^2)ρ, ranging from -0.04 to 0.02 au. Blue indicates strong attractive interactions, and red indicates strong nonbonding overlap

the C-C or C-N bond. It follows that, in the concerted process, C3-N4 bond forming is more advanced than bond N1-C5. Hence, the reaction pathway is in-between a concerted and a stepwise process which can be described generally as an asynchronous concerted one.

The mechanism of the model 1,3-dipolar cycloaddition reaction was also explored by QCISD with 6-31++G(d,p) basis set. It can be concluded from the geometry parameters that the structures of all the stationary points are similar to those at B3LYP/6-31++G(d,p) level. The largest difference in bond length is 0.79 Å for C3-C4 distance in **COMa**, and the maximum difference in bond angle is about 7.4° for the angle C4-C3-N2 in **COMa** (see Tables S1 and S2 in the online resource 1).

The schematic potential energy surface at B3LYP/6-31++G(d,p) level for the model 1,3-dipolar cycloaddition reaction is given in Fig. 3. From this it can be inferred that all the stationary points are lower than the reactant asymptote. Along the concerted pathway, the energy of **TS13a** is 1.96 kcal mol^{-1} higher than **COMa**, but 2.83 kcal mol^{-1} lower than the reactants **R1a** + **R2a**. The potential energy surfaces calculated at QCISD/6-31++G(d,p) and CCSD(T)/6-31++G(d,p)//B3LYP/6-31++G(d,p) levels are also shown in Fig. 3, from which it can be seen that they are very similar for the different calculations (see Table S3 in the online resource 1). The activation barrier for the 1,3-dipolar cycloaddition is only about 0.49 kcal mol^{-1} lower at QCISD/6-31++G(d,p) level and

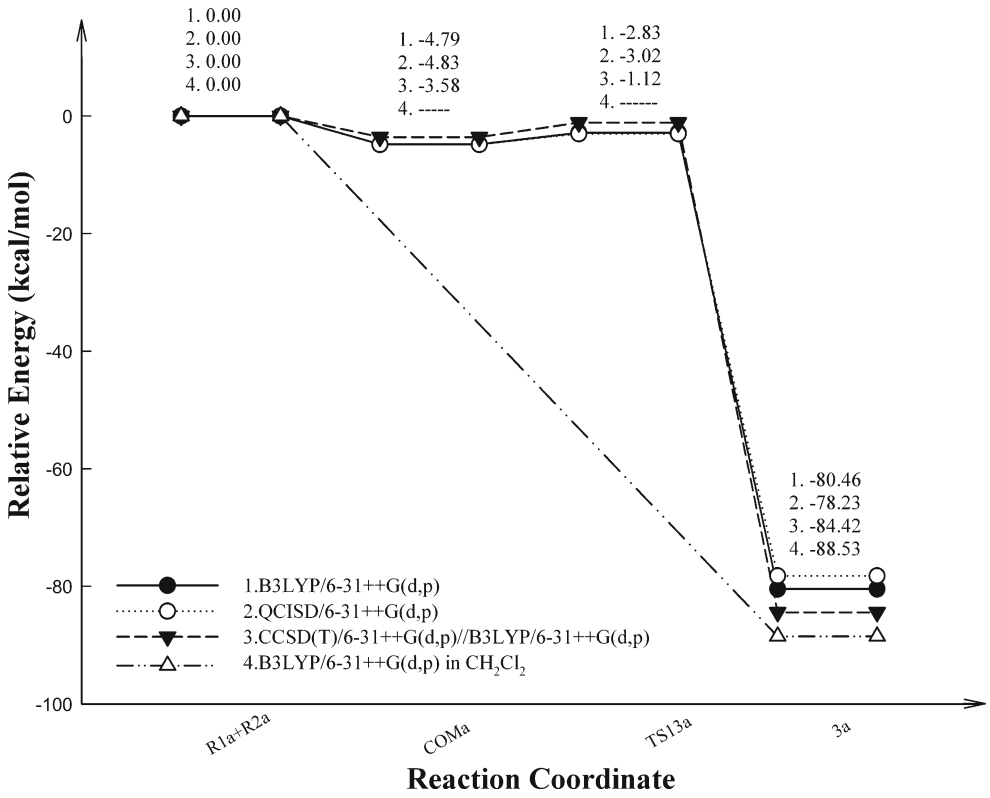

Fig. 3 The schematic potential energy surfaces for the mechanism of the 1,3-dipolar cycloaddition model reaction **R1a** + **R2a** in gas phase

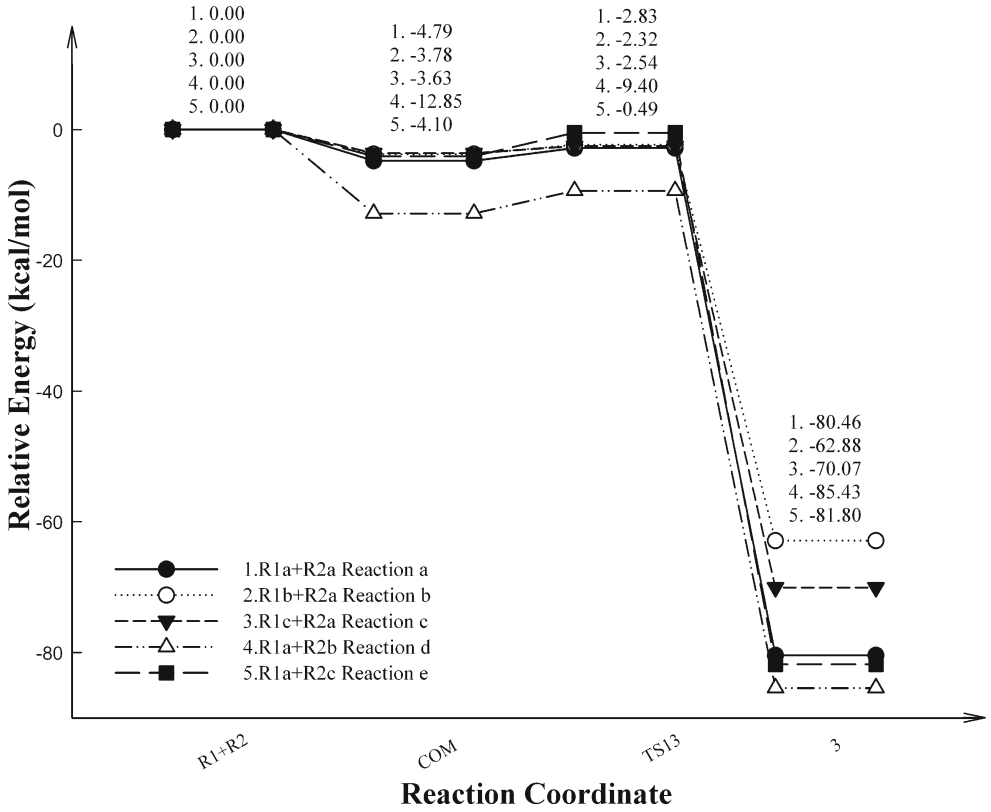

Fig. 4 The schematic potential energy surfaces (with ZPE correction) for the 1,3-dipolar cycloaddition reactions **a**–**e** in gas phase

0.15 kcal mol^{-1} higher at CCSD(T)/6-31++G(d,p)//B3LYP/6-31++G(d,p) level than that at B3LYP/6-31++G(d,p) level.

Substituent effect of the 1,3-dipolar cycloaddition reactions

In this section, the effect of substitution on both azocarbenium ion and acetylene was considered. Methyl and Cl atom were used as representative substituents, and the corresponding reactions are denoted as reaction **b** (**R1b** + **R2a**), **c** (**R1c** + **R2a**), **d** (**R1a** + **R2b**) and **e** (**R1a** + **R2c**) (Scheme 1), respectively. The geometry optimization were performed by B3LYP/6-31++G(d,p) method for all the stationary points, which are denoted as **COMb-e**, **TS13b-e**, and **3b-e**. The schematic potential energy surfaces in gas phase for reactions **b-e** are given in Fig. 4 and the selected bonds and angles of all the transition states are listed in Table 2. The optimized geometric parameters, energies, and frequencies for the reactants are provided in Tables S4-S7, S8 and S9 of the online resource 1. The atomic numbering systems of the above stationary points and more detailed information are given in Figs. S2-S5 (online resource 2). Figure S6 also provides the optimized geometries (B3LYP/6-31++G(d,p)) and gradient isosurfaces (s=1/2 a.u.) for the complexes (**COM**) and the transition states (**TS13**) in reactions **b-e**.

As shown in Table 1, the chemical substitution by methyl on the carbon atom of **R1a** decreases the electrophilicity of **R1b** (ω=11.76), while chlorine substitution increases the electrophilicity of **R1c** (ω=16.09). On the other hand, methyl on the carbon atom of **R2a** (N=1.89) enhances the nucleophilicity index of **R2b** (N=2.78), while chlorine substitution diminishes the nucleophilicity index of **R2c** (N=1.29). However, due to the rather high electrophilicity of the cations, these substituted acetylenes still behave as nucleophiles in the 1,3-dipolar cycloaddition reaction. Similar to the model reaction, when the acetylenes approach the azocarbenium ions, the complexes via noncovalent interaction denoted as **COMb-e** are formed. Afterward, **COM** is destroyed to afford the 3*H*-pyrazolium ions **3** via **TS13** directly.

When methyl or Cl atom is introduced into the azocarbenium ion **R1a**, as shown in Table 2, similar to the model reaction, the skeleton atoms (N1-N2-C3-C4-C5) of the transition states (**TS13b-c**) are coplanar (all dihedral angles are 0.0°). The skeleton atoms (N1-N2-C3) in all the transition states **TS13b-c** are more bent than in the original azocarbenium ion (**R1**), thus favor the concerted process of the 1,3-

Table 2 The distances (BD, Å), angles (BA °) and dihedral angles (DA, °) of some selected bonds and angles in **TS13b-e** at B3LYP/6-31++G(d,p) level

	BD(Å)		BA(°)	DA(°)
	C3…C4	N1…C5	N1-N2-C3	C3…C4-C5…N1
TS13b	2.320	2.600	134.6	0.0
TS13c	2.504	2.693	132.0	0.0
TS13d	2.982	3.515	166.3	2.2
TS13e	2.230	3.902	141.2	1.3

dipolar cycloaddition. Moreover, compared with the distances of the two forming bonds along the reaction progression, the lengths of C3-C4 are always shorter than N1-C5 in **TS13b-c**. These data may suggest a concerted process for the cycloaddition, with C3-N4 bond formation being more advanced than bond N1-C5.

When methyl or Cl atom is introduced into acetylene **R2a**, the lengths of N1-C5 in **TS13d** and **TS13e** are so long that the N1-C5 interactions should not be interpreted as "forming bonds", which is different from reactions **a-c**. It can be seen from Figs. S2-S5 (online resource 2), that compared with product **3d-e**, the structure of transitions states **TS13d-e** that were lack of Cs symmetry are more like the starting compound **COMd-e**. Thus, **TS13d-e** should predict early transition states for the concerted process of the 1,3-dipolar cycloaddition.

In conclusion, the 1,3-dipolar cycloaddition reaction mechanism can be described as an asynchronous concerted pathway with reverse electron demand irrespective of the substituent nature and position, on azocarbenium ion or acetylene.

As reported in our preceding papers [18, 24], the substituent effect should encompass steric effect. For reactions **b** and **c**, considering the relatively large steric effect of methyl and Cl, the 1-aza-2-azoniaallene cations **R1b** and **R1c** become nonlinear molecules. The angles of the skeleton atoms (N1-N2-C3) are 165.1° and 147.5°, respectively, which should be helpful for two set active sites (N1-C5 and C3-C4) approaching each other. These may imply that large steric effect of the substitution facilitates the 1,3-dipolar cycloaddition. As shown in Fig. 4, the activation barriers for the 1,3-dipolar cycloaddition reactions are 1.46 kcal mol^{-1} (reaction **b**) and 1.09 kcal mol^{-1} (reaction **c**), respectively, both of which are appreciably lower than that of the model reaction (1.96 kcal mol^{-1}). For reactions **d** and **e**, the large steric effect of methyl and Cl at the carbon atom of acetylene makes two reactants approach each other more difficultly, thus it disfavors the 1,3-dipolar cycloaddition. As shown in Fig. 4, the activation barriers of 3.45 kcal mol^{-1} (reaction **d**) and 3.61 kcal mol^{-1} (reaction **e**) are all indeed appreciably higher than that of the model reaction (1.96 kcal mol^{-1}). From the above analysis, conclusions can be made that the steric effect of substituents plays a significant role on affecting the 1,3-dipolar cycloaddition.

Solvation effect of the 1,3-dipolar cycloaddition reactions

In this section, we tried to investigate the solvation effect on the above 1,3-dipolar cycloaddition reactions **a-e**. The effect of solvation on the reaction energetics was investigated at B3LYP/6-31++G(d,p) level with a relative permittivity of 8.93 for CH_2Cl_2 that has been fluently employed as the solvent for the experimental work at -60 °C [22]. The relative energies of the stationary points for reactions **a-e** in CH_2Cl_2 are given in Table 3 and the corresponding detailed total energies are listed in Table S8. It can be seen that, 1-aza-2-azoniallene cation **R1** in the solution phase is much more stable than that in the gas phase, which is in good agreement with the fact that 1-aza-2-azoniallene cation **R1** is decomposed during evaporation of the solvent as described by Wang et al. [16]. Moreover, the relative energy of the cycloaddition products **3** in the solution phase is lower than that in the gas phase, complexes (**COMa-e**) and transition states (**TS13a-e**) in solution are less stable than that of the reactants, which means that they will disappear in the solution phase, and the 1,3-doipolar cycloaddition reaction should be a simple ionic reaction to yield more stable cycloadducts **3a-e** along spontaneous process. This is in accord with the experimental finding, described by Wang et al., that cycloaddition of 1-aza-2-azoniaalene salts with acetylenes occurred at -60 °C [22]. Similar results have also been obtained for reactions with other dipolarophiles [18, 20, 24, 26].

The [1,2]-shift reactions

The reaction discrepancy for acetylenes from other dipolarophiles like nitriles, carbodiimides, olefins and isocyanates has been experimentally investigated. It has been disclosed that the outcome of the two-step reaction is not always a single product [22]. The initial product **3** of the above 1,3-dipolar cycloaddition reaction will undergo a consecutive [1,2]-shift reaction to provide 1*H*-pyrazolium salts **4**, 4*H*-pyrazolium salts **5** or mixtures of them. In this section, we investigate the model [1,2]-shift reaction (reaction **a** in Scheme 1) and the substituent effects of the 1-aza-2-azoniaallene cation (reactions **b-c** in Scheme 1) and acetylene (reactions **d-e** in Scheme 1). In order to get more reasonable relative energies of the stationary points at potential energy surfaces, the effect of solvation on the reaction energetics was investigated using PCM with a relative permittivity of 8.93 for CH_2Cl_2 at 0 °C. Figure 5 provides the schematic potential energy surface for the [1,2]-shift reactions in the solution phase. Based on the calculation result, the [1,2]-shift is a kinetically controlled process to afford more stable products **4**/**5**. The optimized parameters, energies, and frequencies of these stationary points are provided in Tables S4-S7, S8 and S9 of the online

Table 3 The relative energies of all the stationary points for 1,3-dipolar cycloaddition reactions **a-e** at B3LYP/6-31++G(d,p) level in CH_2Cl_2

	R	COM	TS13	3
Reaction a	0.00	0.59	6.66	−88.53
Reaction b	0.00	0.48	10.74	−61.94
Reaction c	0.00	1.41	5.35	−72.23
Reaction d	0.00	0.30	1.24	−85.79
Reaction e	0.00	1.68	1.42	−88.86

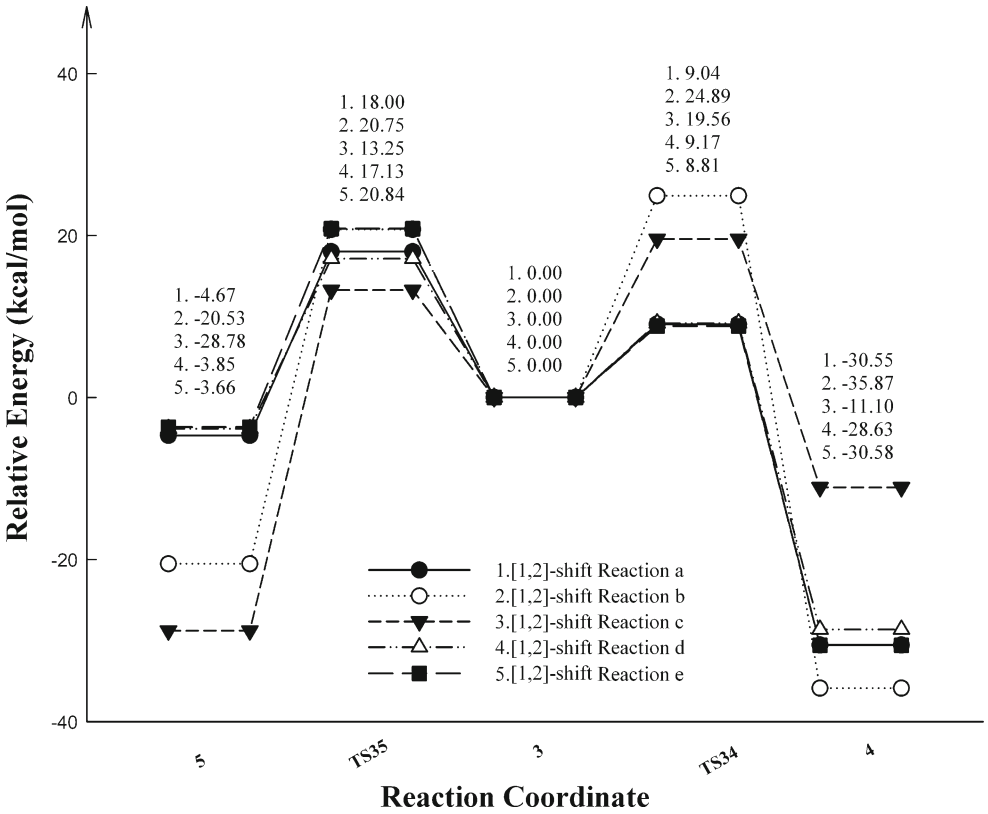

Fig. 5 The schematic potential energy surfaces (with ZPE correction) for the [1,2]-shift reaction **a-e** in solution phase

resource 1. The atomic numbering systems of the above stationary points and more detailed information are gathered in Figs. S1-S5 (online resource 2).

The model [1,2]-shift reaction

The model [1,2]-shift reaction was investigated firstly. Two possible pathways are considered: one is H10 shifting to N2 to produce compound **4a** via **TS34a**, the other one is H10 shifting to C4 to afford compound **5a** via **TS35a**. As shown in Fig. 5, the former way is more favored by 8.96 kcal mol^{-1} than the latter one. We can predict that the 1*H*-pyrazolium salt **4a** should be the major product of the model [1,2]-shift reaction. In order to reach a deeper insight into the mechanism of the [1,2]-shift reaction, we studied carefully all the stationary points, especially for the transition states **TS34a** and **TS35a** along with the different [1,2]-shift reaction pathways, by NBO and LOL analysis. The computational mechanism and atomic numbering systems of these stationary points are shown in Fig. 6 (more detailed information is given in Fig. S1 of the online resource 2), the LOL isosurfaces (v_σ=1/2 a.u.) of all the stationary points are also provided in Fig. 6.

The cycloaddition product **3a** is a five-membered heterocycle with N1-N2, N2-C3, C3-C4, C4-C5, and C5-N1 bond lengths being 1.264, 1.448, 1.485, 1.350, 1.414 Å, respectively. All the atoms except for the two hydrogen atoms connected with the methylene group are in the same plane. As shown in Fig. 6, LOL analysis shows that the bond regions of C4-C5 and N1-N2 in **3a** have a distinct shape and extend strongly into the π-region above and below the bond axis, which are considerably more concave in the case of multiple bonds. In contrast, the bond regions of N2-C3, C3-C4 and C5-N1 are circular cross sections and extend into the σ-region to some extent, so the bonds carry very little double-bond character. Similar to **3a**, **5a** is also a five-membered heterocycle with all the atoms in the same plane except for the two hydrogen atoms connected with the methylene group. However, some deviation in the bond lengths in the main ring fragment can be found. Thus, the bond lengths of N1-N2 and C4-C5 is 1.414 and 1.482 Å, longer by about 0.15 Å and 0.13 Å than their counterparts in **3a**, respectively. This indicates that those bonds turn from typical double bonds in **3a** into single bonds in **5a**. On the other hand, N2-C3 and N1-C5 in **5a** are changed into typical double bonds (N2-C3=1.291 Å, N1-C5=1.294 Å in **5a**) from single bonds with very little double-bond character in **3a**. Moreover, the bond length of C3-C4, 1.499 Å, shows no much difference from that in **3a**. For the other product **4a**, all the atoms are in the same plane with the N1-N2, N2-C3, C3-C4, C4-C5, and C5-N1 bond lengths being 1.352, 1.345, 1.393, 1.393, 1.345 Å, respectively, which exhibits that all bonds in the main ring frame are single bonds with some double-bond character. Additionally, the almost equal bond lengths in **4a** indicates that it has a higher degree of conjugation than product **5a**, which is in agreement with that the relative energy of 1*H*-pyrazolium salt **4a** is 25.88 kcal mol^{-1} more stable than that of 4*H*-pyrazolium salt **5a**.

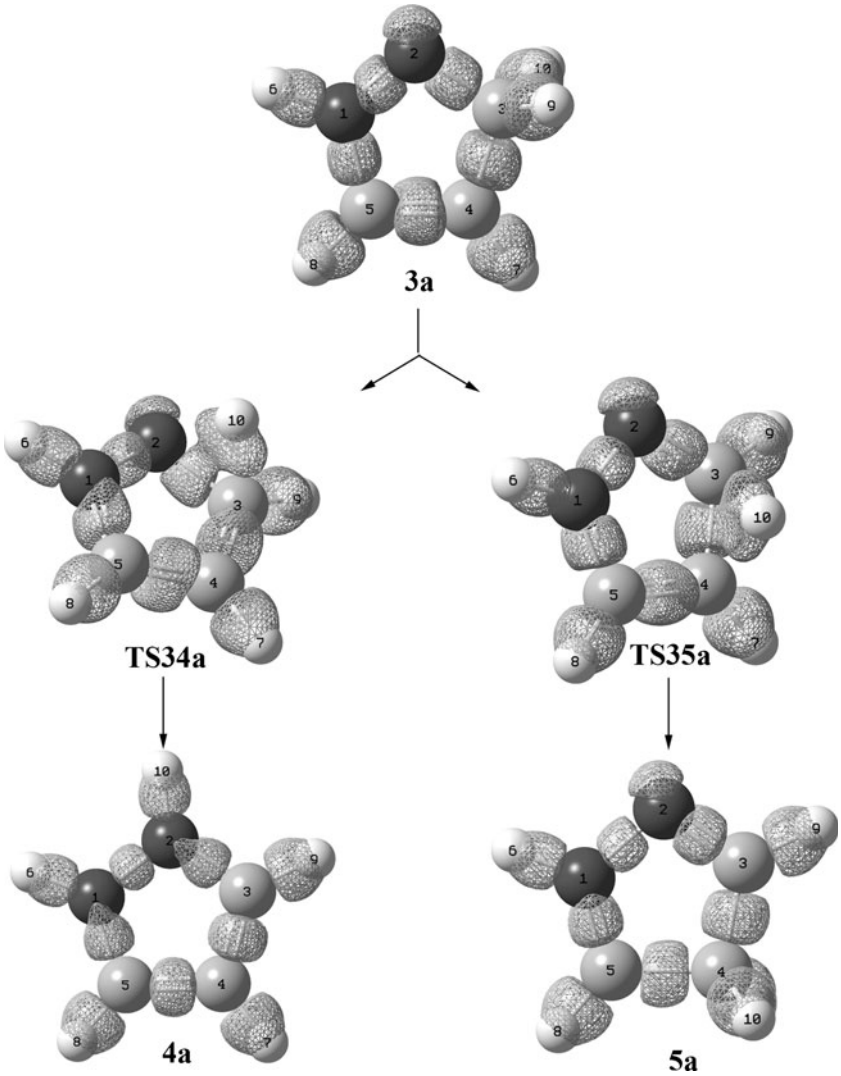

Fig. 6 Optimized geometries (B3LYP/6-31++G(d,p)) and LOL isosurfaces (v_σ=1/2 a.u.) for all the stationary points on the [1,2]-shift model reaction along two different pathways

From **3a** to **4a**/**5a**, with the [1,2]-shift reaction progression, the migrating group H10 shifts from C3 to N2-C3 (C3-C4) bond regions and forms the transition state **TS34a** (**TS35a**). LOL analysis of the **TS**s indicates that the electrons transfer from π orbital of N2-C3 (C3-C4) bond to the electron-deficient orbit of H10 (the natural charge on H10 in **TS34a** and **TS35a** are 0.46 e and 0.42 e, respectively). Thus, the π-electron cloud is deformed and expressed as a T-shaped configurations of v_σ=1/2 a.u. region, in which, the bond regions around the migrating group corresponds to σ-region with a circular cross section and the bond regions around five-membered ring plane corresponds to π-region with distinct shape. At the same time, from **3a** to transition state **TS34a**, the single bonds (N2-C3, C3-C4 and C5-N1) attain the characteristic concave shape of double bonds, and the double bonds (C4-C5 and N1-N2) become more round in shape as they are reduced to single σ-bonds. This is in line with the NBO analysis result that the N2-C3 bond in **TS34a** belongs to a typical double bond. At the same time, π(N2-C3)→*LP**(H10), gives the strongest charge transfer stabilization energies (ΔE_{CT}^2), 339.64 kcal mol^{-1} and the activation barrier for the rearrangement is 9.04 kcal mol^{-1}. Whereas, the composition of natural hybrid orbitals (NHOs) of C3-C4 is C3($sp^{2.53}$)+C4($sp^{2.34}$) from NBO analysis of **TS35a,** suggesting that C3-C4 is a single bond with some double-bond character. Thus the electron density at C3-C4 bond in **TS35a** should be lower than that at double-bond N2=C3 in **TS34a.** Consequently, the strongest charge transfer stabilization energy (ΔE_{CT}^2), π(C3-C4)→*LP**(H10), is only 42.34 kcal mol^{-1} and the activation energy of **TS35a** is 18.00 kcal mol^{-1}, which is almost twice that of **TS34a**. Upon the above analysis of barrier height, NBO and LOL, we can tentatively envision that the 1*H*-pyrazolium salt (**4a**) is the major product in the model [1,2]-shift reaction.

Substituent effect of the [1,2]-shift reactions

Next, the substituent effects in the [1,2]-shift reaction were investigated. The electron-releasing methyl group and electron-withdrawing Cl group were taken as representative

substituents. The corresponding reactions are denoted as reactions **b**, **c**, **d** and **e** as well, similar with the 1,3-dipolar cycloaddition (Scheme 1), and the stationary points are denoted as **3b-e**, **TS34b-e**, **TS35b-e**, **4b-e** and **5b-e**, respectively. The schematic potential energy surface for reactions **b-e** is also given in Fig. 5. Figure 7 provides the optimized geometries and LOL isosurfaces (v_σ=1/2 a.u.) of different transition states (**TS34b-c** and **TS35b-c**) for reactions **b** and **c**.

Based on the calculated results provided in Fig. 5, it can be seen that the type of the migrating group (H, Me or Cl) determines the sense of the [1,2]-shift reaction. When the migrant is H, regardless that the substituent on acetylene is methyl (reaction **d)** or Cl (reaction **e)**, the substituent has only a little influence on the [1,2]-shift reaction. Similar with the model [1,2]-shift reaction, the migrating group H10 regioselectively shifts from C3 to N2 and formation of the corresponding 1*H*-pyrazolium salts (**4d-e**) is the preferred process. When migrating group is methyl (reaction **b)** or Cl (reaction **c),** the migrating terminal turns to C4 rather than C3, and the corresponding 4*H*-pyrazolium salts (**5d-e**) are the predominating products. Especially, the calculated result of reaction **b** (migrating group is methyl) coincides with the experiment findings as described in reference [22]. It also can be explained by the NBO and LOL analysis as the following.

For reaction **b**, NBO analysis shows that the natural charges on the migrating group (methyl) in **TS34b** and **TS35b** are 0.42 e and 0.36 e, respectively. Furthermore, the migrating group methyl in the transition states (**TS34b** and **TS35b**) adopts a triangle pyramid geometry (Fig. 7). The bond angle in the migrating methyl is approximately 115.0°, which means that it should have some carbocation character. And the electron-deficient *p* orbit of C10 will attract and deform the π orbital of N2-C3 or C3-C4, expressed in a T-shaped configuration similar with the model reaction (Fig. 7). NBO analysis also shows that the composition of natural hybrid orbitals (NHOs) of C3-C4 in **TS35b** is C3($sp^{2.09}$)+C4($sp^{2.18}$). Compared with N2($sp^{1.98}$)+C3($sp^{2.99}$) in another transition state **TS34b**, the larger electron density at C3-C4 bond will reinforce the interaction between five-membered ring fragment and the migrating group ($\pi \rightarrow p^*$). This is in good agreement with the large and sharp region of the LOL isosurfaces between the methyl and the five-membered ring residue in **TS35b**. As a result, the stronger interaction will stabilize **TS35b** and then favor the formation of **5b**. As shown in Fig. 5, the activation barrier is 20.75 kcal mol^{-1}, which is lower

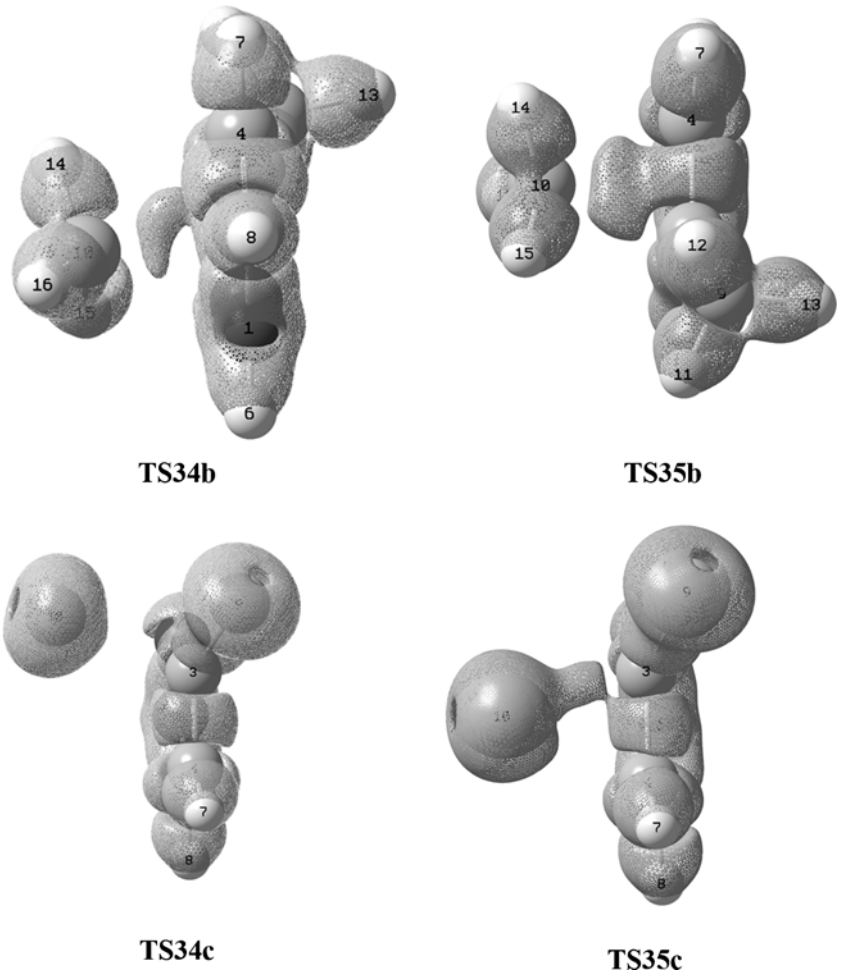

Fig. 7 The optimized geometries (B3LYP/6-31++G (d,p)) and LOL isosurfaces (v_σ=1/2 a.u.) of different transition states (**TS34b-c** and **TS35b-c**) for [1,2]-shift reactions **b** and **c** along two different pathways

by 4.14 kcal mol^{-1} than that for the rearrangement from **3b** to **4b**. On the basis of the above analysis, we can envision that, 4*H*-pyrazolium salts **5b** is the main product for reaction **b**. To sum up, when methyl group is introduced to the carbon atom of **R1a**, substituent will affect the distribution of electron density at the five-membered ring fragment, even the interactions between the five-membered ring and the migrating group in the transition states. Thus, the migrating group methyl regioselectively shifts from C3 to C4 to provide **5b** as the main product.

For reaction **c**, the natural charge on the migrating group Cl in the transition states are 0.20 e, which is the smallest one among all the [1,2]-shift reactions. As shown in Fig. 7, there is a distinguishable lone-pair region around the Cl in the transition states (**TS34c** and **TS35c**). Unlike H or methyl, Cl atom can present some electron-releasing character and alter the electron cloud extending direction. The opposite interaction direction compared with **TS34b** (**TS35b**), from the migrating group Cl10 to the five-membered ring, was observed by LOL analysis. Furthermore, compared with **TS34c**, the region of the LOL isosurfaces between the five-membered ring fragment and Cl10 in **TS35c** is larger and sharper, which means that the interaction between the two fragments in **TS35c** become stronger than that in **TS34c**. Thus, **TS35c** is stabilized and the corresponding activation barrier is 13.25 kcal mol^{-1}, dramatically lower than that for **TS34c** by 6.31 kcal mol^{-1}. On the basis of the calculation result, one can predict that reaction **c** affords the 4*H*-pyrazolium salts **5c** as the main product.

When the substituent (methyl or Cl) is introduced to acetylene, as shown in Fig. 5, the activation barriers for the shifting reactions **d** and **e** are nearly the same as that for the model reaction. This indicates that the substituent group on acetylene **R2a** will not switch the shift direction, the migrating group (H) will always regioselectively shift from C3 to N2, and the 1*H*-pyrazolium salts (**4d** and **4e**) with lower activation barriers are the main products. For detailed and more advanced analysis, when the substituent is methyl (reaction **d**), the activation barrier for the rearrangement from **3d** to **5d** is 7.96 kcal mol^{-1} higher than that for the rearrangement from **3d** to **4d**. The activation barrier difference between two TSs is smaller than that for the model reaction (8.96 kcal mol^{-1}). This means that, in essence, methyl substitution on acetylene is beneficial for the formation of product **5d**. On the other hand, when Cl is introduced to acetylene (reaction **e**), the activation barrier difference 12.03 kcal mol^{-1} between two TSs is larger than that for the model reaction (8.96 kcal mol^{-1}), predicting that Cl on acetylene favors the formation of product **4e**.

Conclusions

In summary, the title reaction, 1,3-dipolar cycloaddition reactions between 1-aza-2-azoniaallene cations and acetylenes and the subsequent [1,2]-shift reaction, have been investigated at B3LYP/6-31++G(d,p) level, and the following conclusions can be drawn:

(1) The title reaction features a tandem reaction that comprises two consecutive processes: an initial ionic 1,3-dipolar [3+2] cycloaddition reaction between 1-aza-2-azoniallene cation and acetylenes to yield the cycloadduct **3** followed by a [1,2]-shift to yield heterocycles **4** and/or **5** depending on the combination of reactants.

(2) For all the studied cycloaddition reactions in gas phase, they can be described as a concerted but asynchronous pathway with reverse electron demand. In CH_2Cl_2 solution, the 1,3-dipolar cycloaddition reaction yields the 3*H*-pyrazolium adducts **3** directly along spontaneous ionic process.

(3) Irrespective of the substituent being electron-releasing methyl, or electron-withdrawing Cl, the activation barriers for the cycloaddition reactions are quite low and the rate-determining step is always the [1,2]-shift process, which is in agreement with the experimental observations.

(4) The subsequent [1,2]-shift reactions are a kinetically controlled process, in which initial products **3** undergo [1,2]-shift reaction to afford more stable products **4**/**5**. The type of the migrating group exhibits dramatic influence on the sense of the migration. When the migrant is H (model reaction and reactions **d**, **e**), it will regioselectively shifts from C3 to N2 and the corresponding 1*H*-pyrazolium salts are the predominating products. When the migrating group is methyl or Cl (reactions **b** and **c**), the migrating terminal will be C4, and the formation of corresponding 4*H*-pyrazolium salts (**5**) becomes favored.

Acknowledgments We acknowledge the assistance of other members of Professor Quan-rui Wang's group for obtaining experimental information. This work was supported by the National Natural Science Foundation of China (No. 21102019) and the Science Fund for Distinguished Young Scholars at Fudan University.

References

1. Huisgen R (1963) 1,3-Dipolar cycloadditions. Past and future. Angew Chem Int Edit 2(10):565–598
2. Padwa A, Pearson WH (2002) Synthetic applications of 1,3 dipolar cycloaddition chemistry toward heterocycles and natural products. Wiley, New York
3. Moura NMM, Giuntini F, Faustino MAF, Neves M, Tome AC, Silva AMS, Rakib EM, Hannioui A, Abouricha S, Roder B, Cavaleiro JAS (2010) 1,3-Dipolar cycloaddition of nitrile imines to meso-tetraarylporphyrins. ARKIVOC (Part 5):24-33
4. Song Z, He XP, Jin XP, Gao LX, Sheng L, Zhou YB, Li J, Chen GR (2011) 'Click' to bidentate bis-triazolyl sugar derivatives with promising biological and optical features. Tetrahedron Lett 52 (8):894–898

5. Cases M, Duran M, Sole M (2000) The [2+1] cycloaddition of singlet oxycarbonylnitrenes to C 60. J Mol Model 6(2):205–212. doi:10.1007/s0089400060205
6. Kuznetsov ML, Kukushkin VY, Dement'Ev AI, Pombeiro AJL (2003) 1,3-dipolar cycloaddition of nitrones to free and Pt-bound nitriles. A theoretical study of the activation effect, reactivity, and mechanism. J Phys Chem A 107(31):6108–6120
7. Meng LP, Wang SC, Fettinger JC, Kurth MJ, Tantillo DJ (2009) Controlling selectivity for cycloadditions of nitrones and alkenes tethered by benzimidazoles: combining experiment and theory G-3263-2010. Eur J Org Chem 2009(10):1578–1584
8. Saeed A, Al-Masoudi NA, Ahmed AA, Pannecouque C (2011) New substituted thiazol-2-ylidene-benzamides and their reaction with 1-Aza-2-azoniaallene salts. Synthesis and anti-HIV activity. Z Naturforsch 66(5):512–520
9. Weingarten MD, Prein M, Price AT, Snyder JP, Padwa A (1997) Theoretical insights regarding the cycloaddition behavior of push-pull stabilized carbonyl ylides. J Org Chem 62(7):2001–2010
10. Kuznetsov ML (2006) Theoretical studies of [3+2]-cycloaddition reactions. USPEKHI KHIMII 75(11):1045–1073
11. Gaich T, Baran PS (2010) Aiming for the ideal synthesis. J Org Chem 75(14):4657–4673
12. Meng Q, Li M (2012) Theoretical studies on the Mo-catalyzed asymmetric intramolecular Pauson-Khand-type [2+2+1] cycloadditions of 3-allyloxy-1-propynylphosphonates. J Mol Model doi:10.1007/s00894-012-1361-z
13. Houk KN, Firestone RA, Munchausen LL, Mueller PH, Arison BH, Garcia LA (1985) stereospecificity of 1,3-dipolar cycloadditions of para-nitrobenzonitrile oxide to cis-dideuterioethylene and trans-dideuterioethylene. J Am Chem Soc 107(24):7227–7228
14. Di Valentin C, Freccero M, Gandolfi R, Rastelli A (2000) Concerted vs stepwise mechanism in 1,3-dipolar cycloaddition of nitrone to ethene, cyclobutadiene, and benzocyclobutadiene: a computational study. J Org Chem 65(19):6112–6120
15. Ponti A, Molteni G (2001) DFT-based quantitative prediction of regioselectivity: cycloaddition of nitrilimines to methyl propiolate. J Org Chem 66(15):5252–5255
16. Wang QR, Jochims JC, Kohlbrandt S, Dahlenburg L, Altalib M, Hamed A, Ismail AEH (1992) 1,2,4-triazolium salts from the reaction of 1-aza-2-azoniaallene salts with nitriles. Synth Stuttgart 24(7):710–718
17. Wirschun W, Winkler M, Lutz K, Jochims JC (1998) 1,3-diaza-2-azoniaallene salts: cycloadditions to alkynes, carbodiimides and cyanamides. J Chem Soc Perk T 1(11):1755–1761
18. Li ZM, Wang QR (2008) A theoretical investigation on the cycloaddition reaction between azocarbenium ions and nitriles. Int J Quantum Chem 108(6):1067–1075
19. Wirschun W, Jochims JC (1997) 1,3-diaza-2-azoniaallene salts, novel N-3-building blocks: Preparation and cycloadditions to olefins. Synth Stuttgart 29(2):233–241
20. Wei MJ, Fang DC, Liu RZ (2002) Theoretical studies on cycloaddition reactions between 1-aza-2-azoniaallene cation and olefins. J Org Chem 67(21):7432–7438
21. Abuelhalawa R, Jochims JC (1992) on the reaction of n-alkylnitrilium salts with acetylenes - a new synthesis of 2-azoniaallene salts. Synth Stuttgart 24(9):871–874
22. Wang QR, Altalib M, Jochims JC (1994) On the reaction of 1-aza-2-azoniaallene salts with acetylenes. Chem Ber 127(3):541–547
23. Wang QR, Amer A, Troll C, Fischer H, Jochims JC (1993) On the reaction of 1-aza-2-azoniaallene salts with carbodiimides. Chem Ber 126(11):2519–2524
24. Wang JM, Li ZM, Wang QR, Tao FG (2012) A DFT study on the mechanisms for the cycloaddition reactions between 1-Aza-2-azoniaallene cations and carbodiimides. Int J Quantum Chem 112 (3):809–822. doi:10.1002/qua.23065
25. Wang QR, Mohr S, Jochims JC (1994) On the reaction of 1-aza-2-azoniaallene salts with isocyanates. Chem Ber 127(5):947–953
26. Wei MJ, Fang DC, Liu RZ (2004) Theoretical studies on cycloaddition reactions between 1-aza-2-azoniaallene cations and isocyanates. Eur J Org Chem 2004(19):4070–4076
27. Wyman J, Javed MI, Al-Bataineh N, Brewer M (2010) Synthetic approaches to bicyclic diazenium salts. J Org Chem 75(23):8078–8087
28. Frisch MJ, Trucks GW, Schlegel HB, Scuseria GE, Robb MA, Cheeseman JR, Scalmani G, Barone V, Mennucci B, Petersson GA, Nakatsuji H, Caricato M, Li X, Hratchian HP, Izmaylov AF, Bloino J, Zheng G, Sonnenberg JL, Hada M, Ehara M, Toyota K, Fukuda R, Hasegawa J, Ishida M, Nakajima T, Honda Y, Kitao O, Nakai H, Vreven T, Montgomery JA Jr, Peralta JE, Ogliaro F, Bearpark M, Heyd JJ, Brothers E, Kudin KN, Staroverov VN, Kobayashi R, Normand J, Raghavachari K, Rendell A, Burant JC, Iyengar SS, Tomasi J, Cossi M, Rega N, Millam NJ, Klene M, Knox JE, Cross JB, Bakken V, Adamo C, Jaramillo J, Gomperts R, Stratmann RE, Yazyev O, Austin AJ, Cammi R, Pomelli C, Ochterski JW, Martin RL, Morokuma K, Zakrzewski VG, Voth GA, Salvador P, Dannenberg JJ, Dapprich S, Daniels AD, Farkas, Foresman JB, Ortiz JV, Cioslowski J, Fox DJ (2009) Gaussian 09, A.02nd edn. Gaussian Inc, Wallingford
29. Gonzalez C, Schlegel HB (1989) An improved algorithm for reaction-path following. J Chem Phys 90(4):2154–2161
30. Gonzalez C, Schlegel HB (1990) Reaction-path following in mass-weighted internal coordinates. J Org Chem 94(14):5523–5527
31. Gauss J, Cremer D (1988) Analytical evaluation of energy gradients in quadratic configuration interaction theory. Chem Phys Lett 150(3–4):280–286. doi:10.1016/0009-2614(88)80042-3
32. Salter EA, Trucks GW, Bartlett RJ (1989) Analytic energy derivatives in many-body methods. I. First derivatives. J Chem Phys 90 (3):1752–1766
33. Watts JD, Gauss J, Bartlett RJ (1992) Open-shell analytical energy gradients for triple excitation many-body, coupled-cluster methods: MBPT(4), CCSD+T(CCSD), CCSD(T), and QCISD(T). Chem Phys Lett 200(1–2):1–7. doi:10.1016/0009-2614(92)87036-o
34. Scuseria GE (1991) Analytic evaluation of energy gradients for the singles and doubles coupled cluster method including perturbative triple excitations: theory and applications to FOOF and Cr[sub 2]. J Chem Phys 94(1):442–447
35. Miertus S, Scrocco E, Tomasi J (1981) Electrostatic interaction of a solute with a continuum - a direct utilization of abinitio molecular potentials for the prevision of solvent effects. Chem Phys 55 (1):117–129
36. Barone V, Cossi M, Tomasi J (1997) A new definition of cavities for the computation of solvation free energies by the polarizable continuum model. J Chem Phys 107(8):3210–3221
37. Cances E, Mennucci B, Tomasi J (1997) A new integral equation formalism for the polarizable continuum model: theoretical background and applications to isotropic and anisotropic dielectrics. J Chem Phys 107(8):3032–3041
38. Cossi M, Barone V, Mennucci B, Tomasi J (1998) *Ab initio* study of ionic solutions by a polarizable continuum dielectric model. Chem Phys Lett 286(3–4):253–260
39. Perez P (2004) Relationship between superelectrophilicity and the electrophilicity index of isolated species. J Org Chem 69 (15):5048–5053. doi:10.1021/jo049945f
40. Noorizadeh S, Shakerzadeh E (2008) A new scale of electronegativity based on electrophilicity index. J Phys Chem A 112 (15):3486–3491. doi:10.1021/jp709877h
41. Chattaraj PK, Giri S, Duley S (2011) Update 2 of: electrophilicity index. Chem Rev 111(2):PR43–PR75. doi:10.1021/cr100149p
42. Chattaraj PK, Duley S, Domingo LR (2012) Understanding local electrophilicity/nucleophilicity activation through a single reactivity difference index. Org Biomol Chem 10(14):2855–2861. doi:10.1039/c2ob06943a

43. Domingo LR, Chamorro E, Perez P (2008) Understanding the reactivity of captodative ethylenes in polar cycloaddition reactions: a theoretical study. J Org Chem 73(12):4615–4624. doi:10.1021/jo800572a
44. Glendening ED, Badenhoop JK, Reed AE, Carpenter JE, Bohmann JA, Morales CM, Weinhold F, Morales M, Weinhold F (2010) NBO 5.9. Theoretical Chemistry Institute, University of Wisconsin, Madison
45. Yin B, Huang Y, Wang G, Wang Y (2010) Combined DFT and NBO study on the electronic basis of Si···N-β-donor bond. J Mol Model 16(3):437–446. doi:10.1007/s00894-009-0560-8
46. Davari M, Bahrami H, Haghighi Z, Zahedi M (2010) Quantum chemical investigation of intramolecular thione-thiol tautomerism of 1,2,4-triazole-3-thione and its disubstituted derivatives. J Mol Model 16(5):841–855. doi:10.1007/s00894-009-0585-z
47. Jacobsen H (2008) Localized-orbital locator (LOL) profiles of chemical bonding. Can J Chem 86(7):695–702
48. Jacobsen H (2009) Chemical bonding in view of electron charge density and kinetic energy density descriptors. J Comput Chem 30 (7):1093–1102. doi:10.1002/jcc.21135
49. Yang Y (2010) Hexacoordinate bonding and aromaticity in silicon phthalocyanine. J Phys Chem A 114(50):13257–13267. doi:10.1021/jp109278v
50. Steinmann SN, Mo Y, Corminboeuf C (2011) How do electron localization functions describe pi-electron delocalization? Phys Chem Chem Phys 13(46):20584–20592. doi:10.1039/c1cp21055f
51. Johnson ER, Keinan S, Mori-Sanchez P, Contreras-Garcia J, Cohen AJ, Yang W (2010) Revealing noncovalent interactions. J Am Chem Soc 132(18):6498–6506. doi:10.1021/ja100936w
52. Lu T (2011) Multiwfn 2.21. School of Chemical and Biological Engineering. University of Science and Technology Beijing, China
53. Reed AE, Curtiss LA, Weinhold F (1988) Intermolecular interactions from a natural bond orbital, donor-acceptor viewpoint. Chem Rev 88(6):899–926. doi:10.1021/cr00088a005
54. Sustmann R (1971) A simple model for substituent effects in cycloaddition reactions. II. The diels-alder reaction. Tetrahedron Lett 12(29):2721–2724. doi:10.1016/s0040-4039(01)96962-x